Mineralogical Magazine, December 2017, Vol. 81(6), pp. 1523–1531

Magnesiocanutite, $NaMnMg_2[AsO_4]_2[AsO_2(OH)_2]$, a new protonated alluaudite-group mineral from the Torrecillas mine, Iquique Province, Chile

ANTHONY R. KAMPF[1,*], BARBARA P. NASH[2], DINI MAURIZIO[3] AND ARTURO A. MOLINA DONOSO[4]

[1] Mineral Sciences Department, Natural History Museum of Los Angeles County, 900 Exposition Boulevard, Los Angeles, CA 90007, USA
[2] Department of Geology and Geophysics, University of Utah, Salt Lake City, Utah 84112, USA
[3] Pasaje San Agustin 4045, La Serena, Chile
[4] Los Algarrobos 2986, Iquique, Chile

[*Received 17 October 2016; Accepted 19 February 2017; Associate Editor: Ian Graham*]

ABSTRACT

The new mineral magnesiocanutite (IMA2016-057), $NaMnMg_2[AsO_4]_2[AsO_2(OH)_2]$, was found at the Torrecillas mine, Iquique Province, Chile, where it occurs as a secondary phase in association with anhydrite, canutite, halite, lavendulan and magnesiokoritnigite. Magnesiocanutite occurs as pale brownish-pink to rose-pink, lozenge-shaped tablets that are often grouped in tightly intergrown aggregates. The crystal forms are {110} and {102}. Crystals are transparent, with vitreous lustre and white to very pale pink streak. The Mohs hardness is 2½, tenacity is brittle, and the fracture is splintery. Crystals exhibit two perfect cleavages: {010} and {101}. The calculated density is 3.957 g/cm^3. Optically, magnesiocanutite is biaxial (+), with $\alpha = 1.689(2)$, $\beta = 1.700(2)$, $\gamma = 1.730(2)$ (measured in white light); $2V_{meas.} = 64.3(4)°$; slight dispersion, $r < v$; orientation $Z = \mathbf{b}$; $X \wedge \mathbf{a} = 15°$ in obtuse angle β. The mineral is slowly soluble in dilute HCl at room temperature. Electron-microprobe analyses, provided Na_2O 5.44, CaO 0.26, MgO 8.84, MnO 18.45, CoO 1.47, CuO 2.13, As_2O_5 59.51, H_2O(calc) 2.86, total 98.96 wt.%. Magnesiocanutite is monoclinic, $C2/c$, $a = 12.2514(8)$, $b = 12.4980(9)$, $c = 6.8345(5)$ Å, $\beta = 113.167(8)°$, $V = 962.10(13)$ Å^3 and $Z = 4$. The eight strongest powder X-ray diffraction lines are [d_{obs} Å(I)(hkl)]: 6.25(42)(020), 3.566(43)(310,$\bar{1}$31), 3.262(96)($\bar{1}$12), 3.120(59)(002,131,040,221), 2.787(93)(400,022,041,330), 2.718(100)($\bar{4}$21,240,112,$\bar{4}$02), 2.641(42)($\bar{1}$32) and 1.5026(43)(multiple). Magnesiocanutite has a protonated alluaudite-type structure ($R_1 = 2.59\%$ for 789 $F_o > 4\sigma F$ reflections) and is the Mg analogue of canutite. Using the results of both the microprobe analyses and structure refinement, the structurally based empirical formula is $Na(Mn_{0.78}Mg_{0.22})_{\Sigma 1.00}(Mg_{1.04}Mn_{0.70}Cu_{0.15}Co_{0.11})_{\Sigma 2.00}[AsO_4]_2[AsO_2(OH)_2]$.

KEYWORDS: magnesiocanutite, new mineral, canutite, arsenate, alluaudite group, crystal structure, Torrecillas mine, Iquique Province, Chile.

Introduction

OVER the last several years, our investigations of the minerals of the Torrecillas mine, a small, long-inactive arsenic mine in the northern Atacama Desert of Chile, have revealed a remarkable assemblage of rare secondary chlorides, arsenates and arsenites, many of which are new mineral species. To date, the descriptions of eight new minerals have been published: the chloride laverettite (Kampf *et al.*, 2013*a*); the arsenates magnesiokoritnigite (Kampf *et al.*, 2013*b*), canutite (Kampf *et al.*, 2014*a*), chongite (Kampf *et al.*, 2016*a*), currierite (Kampf *et al.*, 2017*a*) and juansilvaite (Kampf *et al.*, 2017*b*); and the arsenites torrecillasite (Kampf *et al.*, 2014*b*) and gajardoite

*E-mail: akampf@nhm.org
https://doi.org/10.1180/minmag.2017.081.013

TABLE 1. Comparative data for magnesiocanutite and canutite.

	Magnesiocanutite	Canutite
Ideal formula	$NaMnMg_2[AsO_4]_2[AsO_2(OH)_2]$	$NaMn_3[AsO_4]_2[AsO_2(OH)_2]$
Space group	*C*2/*c*	*C*2/*c*
a (Å)	12.2514(8)	12.3132(5)
b (Å)	12.4980(9)	12.6042(6)
c (Å)	6.8345(5)	6.8717(5)
β (°)	113.167(8)	113.500(8)
V (Å^3)	962.10(13)	978.02(9)
Z	4	4
Density calc (g/cm^3)	3.957	4.119
Optical character	biaxial (+)	biaxial (+)
α	1.689(2)	1.712(3)
β	1.700(2)	1.725(3)
γ	1.730(2)	1.756(3)
2 V (°)	64.3(4)	65.6(4)

(Kampf *et al.*, 2016*b*). Herein, we describe the ninth new mineral from the Torrecillas mine, the alluaudite-group arsenate magnesiocanutite. Several other potentially new minerals are still under study.

Magnesiocanutite is a member of the alluaudite group and is isostructural with compounds with the protonated alluaudite-type structure, which have the general formula $AM1M2_2[T1O_4][T2O_3(OH)]_2$, in which the *A* cations occupy large sites in channels of a framework composed of *M*1 and *M*2 octahedra, and *T*1 and *T*2 tetrahedra. The name magnesiocanutite was chosen to highlight the fact that the mineral is the Mg analogue of canutite, $NaMn_3[AsO_4]_2[AsO_2(OH)_2]$, with Mg rather than Mn dominant in the *M*2 site. The cell parameters, densities and optical properties of canutite and magnesiocanutite are compared in Table 1. Powder X-ray diffraction and energy-dispersive spectroscopy (EDS) indicate that other arsenate members of the alluaudite group containing varying contents of Na, Ca, Mg, Mn, Cu and Fe are also present in the Torrecillas secondary assemblages. Based upon the relatively low temperature of the secondary assemblages and the occurrence of the protonated alluaudite-group minerals canutite and magnesiocanutite, it seems probable that other such alluaudite-group phases are also protonated; however, these phases are difficult to define unambiguously because they are generally not suitable for single-crystal study.

The new mineral and the name have been approved by the International Mineralogical Association (IMA2016-057). The description is based upon one holotype and one cotype specimen that are deposited in the collections of the Natural History Museum of Los Angeles County, 900 Exposition Boulevard, Los Angeles, CA 90007, USA, catalogue numbers 66273 and 66274, respectively.

Occurrence

The new mineral was found at the Torrecillas mine, Salar Grande, Iquique Province, Tarapacá Region, Chile (~20°58'13″S 70°8'17″W). Torrecillas Hill, on which the Torrecillas mine is located, is composed of four different rock units. The Coastal Range Batholith (mainly gabbros) extends from the seashore to the Pan-American Road along the base of Torrecillas Hill. At the foot of Torrecillas Hill is a small area of contact metamorphic rocks in which garnet crystals occur in metamorphosed shales. Higher on the hill, the rocks are predominantly andesites and porphyritic lavas of the Jurassic La Negra Formation. The Torrecillas deposit, in which the new mineral is found, consists of two main veins rich in secondary arsenic and copper minerals that intersect metamorphosed marine shales and lavas. These mineralized veins are related genetically to the aforementioned andesites and porphyritic lavas of the Jurassic La Negra Formation. More information on the geology and mineralogy of the area is provided by Gutiérrez (1975).

The rare secondary chlorides, arsenates and arsenites have been found at three main sites on the hill: an upper pit measuring ~8 m long and

https://doi.org/10.1180/minmag.2017.081.013 Published online by Cambridge University Press

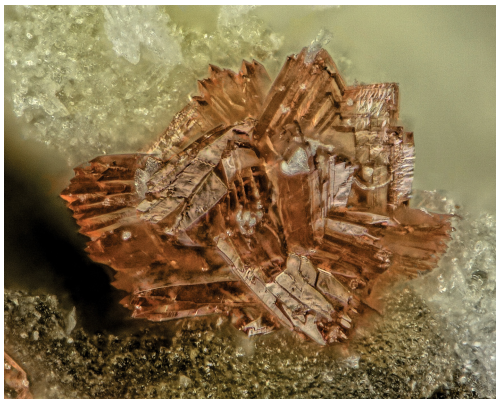

FIG. 1. Intergrown magnesiocanutite crystals. Field of View = 0.45 mm.

3 m deep, a lower pit ~100 m from the upper pit and measuring ~5 m long and 3 m deep, and a mine shaft adjacent to the lower pit and lower on the hill. Magnesiocanutite was found in the upper pit and in the area of the mine shaft by a collecting party consisting of three of the authors (ARK, MD and AAMD) along with Jochen Schlüter and Joe Marty in February 2014.

The new mineral is a secondary phase occurring in association with anhydrite, canutite, halite, lavendulan and magnesiokoritnigite. The secondary assemblages at the Torrecillas deposit are interpreted as having formed from the oxidation of native arsenic and other As-bearing primary phases, followed by later alteration by saline fluids derived from evaporating meteoric water under hyperarid conditions (cf. Cameron *et al.*, 2007).

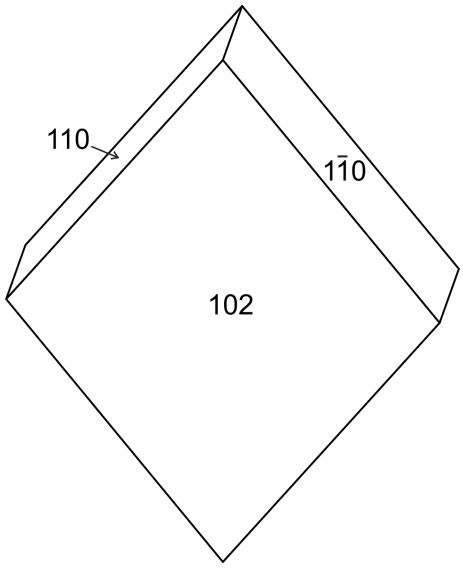

FIG. 2. Crystal drawing of magnesiocanutite, clinographic projection in non-standard orientation, [20$\bar{1}$] vertical.

Physical and optical properties

Magnesiocanutite occurs as pale brownish-pink to rose-pink, lozenge-shaped tablets to ~0.5 mm in maximum dimension. Tablets are often grouped in tightly intergrown aggregates (Fig. 1). The tablets are flattened on {102} and slightly elongated on [20$\bar{1}$]; the crystal forms exhibited are {110} and {102} (Fig. 2). No twinning was observed. Crystals are transparent, with vitreous lustre and white to very pale pink streak. The Mohs hardness is 2½ based upon scratch tests. The tenacity is brittle, and the fracture is splintery as a result of two perfect cleavages, {010} and {101}. Efforts to measure the density by flotation in Clerici solution were unsuccessful because of the difficulty in identifying the most Mg-rich crystal aggregates and the difficulty in observing the aggregates in the solution. The calculated density is 3.957 g/cm^3 based on the empirical formula and 3.764 g/cm^3 based on the ideal formula. The mineral is slowly soluble in dilute HCl at room temperature.

Optically, magnesiocanutite is biaxial (+), with $\alpha = 1.689(2)$, $\beta = 1.700(2)$, $\gamma = 1.730(2)$ determined in white light. The measured 2V is 64.3(4)° based on extinction data collected on a spindle stage and analysed using *EXCALIBRW* (Gunter *et al.*, 2004). The calculated 2V is 63.3°. Slight

TABLE 2. Analytical data (wt.%) for magnesiocanutite.

Constituent	Mean	Min	Max	SD	Standard
Na_2O	5.44	5.21	5.59	0.12	albite
CaO	0.26	0.11	0.31	0.06	diopside
MgO	8.84	8.17	10.35	0.69	diopside
MnO	18.45	16.28	19.60	0.98	rhodonite
CoO	1.47	1.13	1.78	0.18	Co metal
CuO	2.13	1.20	2.75	0.51	Cu metal
As_2O_5	59.51	58.85	60.75	0.55	Syn. GaAs
H_2O*	2.86				
Total	98.96				

* Calculated on the basis of 3 As, charge balance and 12 O apfu. SD – standard deviation.

https://doi.org/10.1180/minmag.2017.081.013 Published online by Cambridge University Press

TABLE 3. Powder X-ray diffraction data for magnesiocanutite.

I_{obs}	d_{obs}	d_{calc}	I_{calc}	$h\ k\ l$	I_{obs}	d_{obs}	d_{calc}	I_{calc}	$h\ k\ l$
4	8.37	8.3670	3	1 1 0			1.7979	2	6 2 0
42	6.25	6.2490	49	0 2 0			1.7793	3	$\bar{5}$ 3 3
21	5.59	5.6317	23	2 0 0			1.7634	5	1 7 0
21	4.42	4.4398	14	1 1 1			1.7593	2	$\bar{4}$ 4 3
33	4.13	4.1835	22	2 2 0			1.7492	3	1 3 3
36	4.03	4.0746	39	$\bar{2}$ 2 1	13	1.7299	1.7257	12	$\bar{1}$ 7 1
13	3.902	3.9073	17	1 3 0			1.7215	3	$\bar{4}$ 6 1
10	3.776	3.7982	10	$\bar{3}$ 1 1			1.7100	2	4 2 2
43	3.566	3.5957	33	3 1 0	32	1.6890	1.6955	26	$\bar{2}$ 0 4
		3.5419	15	$\bar{1}$ 3 1			1.6805	18	$\bar{6}$ 4 2
		3.3639	7	$\bar{2}$ 0 2			1.6734	9	5 5 0
96	3.262	3.2727	100	$\bar{1}$ 1 2	19	1.6666	1.6712	3	1 7 1
		3.1417	20	0 0 2			1.6608	2	$\bar{1}$ 5 3
59	3.120	3.1319	26	1 3 1			1.6463	3	$\bar{4}$ 6 2
		3.1245	13	0 4 0			1.6091	7	6 4 0
		3.0905	11	2 2 1	6	1.6007	1.6023	2	$\bar{7}$ 3 2
19	2.970	2.9887	19	$\bar{3}$ 1 2			1.5959	6	7 1 0
		2.9620	6	$\bar{2}$ 2 2			1.5452	8	4 4 2
		2.8159	28	4 0 0			1.5444	7	$\bar{3}$ 7 2
93	2.787	2.8069	4	0 2 2	23	1.5324	1.5390	2	$\bar{6}$ 0 4
		2.7977	15	0 4 1			1.5371	2	$\bar{2}$ 6 3
		2.7890	57	3 3 0			1.5316	3	$\bar{1}$ 3 4
		2.7463	9	$\bar{4}$ 2 1			1.5287	13	$\bar{8}$ 0 2
100	2.718	2.7322	74	2 4 0			1.5274	3	2 4 3
		2.6935	15	1 1 2			1.5161	4	0 8 1
		2.6871	30	$\bar{4}$ 0 2			1.5117	7	$\bar{5}$ 3 4
42	2.641	2.6299	44	$\bar{1}$ 3 2			1.5104	4	$\bar{7}$ 3 3
18	2.578	2.5673	20	4 2 0	43	1.5026	1.5054	2	2 8 0
		2.4686	3	$\bar{4}$ 2 2			1.5019	15	3 7 1
		2.4028	4	$\bar{5}$ 1 1			1.5010	14	7 3 0
8	2.372	2.3748	11	2 0 2			1.5002	2	$\bar{2}$ 8 1
3	2.296	2.3110	4	3 3 1			1.4988	8	1 7 2
13	2.205	2.2170	17	$\bar{5}$ 1 0			1.4944	2	$\bar{6}$ 2 4
		2.2073	2	$\bar{3}$ 1 3			1.4902	3	$\bar{2}$ 4 4
		2.1853	5	$\bar{4}$ 4 1			1.4849	2	$\bar{8}$ 2 2
4	2.0652	2.0807	8	3 5 0	18	1.4809	1.4810	8	$\bar{4}$ 4 4
		2.0211	20	$\bar{5}$ 3 2			1.4769	2	0 6 3
		2.0188	3	3 1 2			1.4680	2	1 1 4
21	2.0021	2.0151	3	$\bar{4}$ 2 3			1.4542	2	$\bar{6}$ 6 1
		2.0121	2	$\bar{1}$ 5 2			1.4460	4	6 4 1
		1.9934	2	$\bar{6}$ 0 2			1.4336	2	$\bar{7}$ 1 4
		1.9859	5	0 2 3			1.4257	3	$\bar{7}$ 5 2
		1.9816	2	5 3 0			1.4169	2	$\bar{2}$ 8 2
		1.9747	7	$\bar{3}$ 3 3			1.4035	7	0 4 4
26	1.9513	1.9422	4	$\bar{2}$ 6 1			1.3992	5	$\bar{5}$ 7 0
		1.9404	22	$\bar{3}$ 5 2	18	1.3971	1.3968	2	$\bar{1}$ 7 3
13	1.9152	1.9317	5	$\bar{6}$ 2 1			1.3932	4	1 3 4
		1.8991	2	$\bar{6}$ 2 2			1.3919	8	$\bar{3}$ 7 3
		1.8772	3	6 0 0			1.3912	4	$\bar{4}$ 8 1
		1.8580	2	3 5 1			1.3888	7	6 0 2
		1.8522	17	1 5 2	16	1.3813	1.3792	6	2 0 4
34	1.8393	1.8405	6	$\bar{2}$ 4 3			1.3732	4	$\bar{8}$ 4 2
		1.8362	20	3 3 2					

Only calculated lines with intensities of 3 or greater are shown.

https://doi.org/10.1180/minmag.2017.081.013 Published online by Cambridge University Press

$r < v$ dispersion was observed. The optical orientation is $Z = \mathbf{b}$; $X \wedge \mathbf{a} = 15°$ in obtuse angle β. Pleochroism is imperceptible.

Composition

Quantitative analyses (nine points on four crystals) were performed at the University of Utah on a Cameca SX-50 electron microprobe with four wavelength-dispersive spectrometers (WDS) utilizing *Probe for EPMA* software. Analytical conditions were: 15 kV accelerating voltage, 10 nA beam current and a beam diameter of 10 μm. Magnesiocanutite exhibited visible damage under the electron beam. Sodium experienced a time-dependent decrease in intensity under the electron beam, whereas As sustained an increase; both were accounted for by an exponential fit to the intensity *vs*. time measurements and extrapolation to zero-time intensity.

No other elements were detected by EDS. Other possible elements were sought by WDS scans, but none were above the detection limits. Raw X-ray intensities were corrected for matrix effects with a ϕ(ρz) algorithm (Pouchou and Pichoir, 1991). Because insufficient material was available for a direct determination of H_2O, the amount of water was calculated on the basis of 3 As atoms per formula unit (apfu), charge balance and 12 O apfu, as determined by the crystal structure analysis (see below). Analytical data are given in Table 2.

The empirical formula is $(Na_{1.02}Ca_{0.03}Mn_{1.51}Mg_{1.27}Cu_{0.16}Co_{0.11})_{\Sigma 4.10}As_3O_{12}H_{1.84}$. The simplified structural formula is $Na(Mn,Mg)(Mg,Mn)_2[AsO_4]_2[AsO_2(OH)_2]$ and the end-member formula is $NaMnMg_2[AsO_4]_2[AsO_2(OH)_2]$, which requires Na_2O 5.68, MgO 14.78, MnO

TABLE 4. Data collection and structure refinement details for magnesiocanutite.

Diffractometer	Rigaku R-Axis Rapid II
X-ray radiation / power	Mo$K\alpha$ ($\lambda = 0.71075$ Å)/50 kV, 40 mA
Temperature	298(2) K
Structural formula	$Na(Mn_{0.748}Mg_{0.252})_{\Sigma 1.00}(Mg_{1.114}Mn_{0.886})_{\Sigma 2.00}[AsO_4]_2[AsO_2(OH)_2]$
Space group	$C2/c$
Unit cell dimensions	$a = 12.2514(8)$ Å $b = 12.4980(9)$ Å $c = 6.8345(5)$ Å $\beta = 113.167(8)°$
V	962.10(13) Å^3
Z	4
Density (for above formula)	3.899 g/cm^3
Absorption coefficient	12.610 mm^{-1}
$F(000)$	1061
Crystal size (μm)	75 × 45 × 20
θ range (°)	3.26 to 25.03
Index ranges	$-14 \le h \le 12$, $-14 \le k \le 14$, $-8 \le l \le 8$
Refls. collected/unique	4478 / 849; $R_{int} = 0.051$
Reflections with $F_o > 4\sigma F$	789
Completeness to $\theta = 25.03°$	99.3%
Max. and min. transmission	0.787 and 0.451
Refinement method	Full-matrix least-squares on F^2
Parameters refined	93
Goof	1.110
Final R indices [$F_o > 4\sigma(F)$]	$R_1 = 0.0259$, $wR_2 = 0.0542$
R indices (all data)	$R_1 = 0.0286$, $wR_2 = 0.0556$
Largest diff. peak / hole	+0.74 / –0.63 e/A^3

*$R_{int} = \Sigma|F_o^2 - F_o^2(\text{mean})|/\Sigma[F_o^2]$. Goof = $S = \{\Sigma[w(F_o^2 - F_c^2)^2]/(n-p)\}^{1/2}$. $R_1 = \Sigma||F_o| - |F_c||/\Sigma|F_o|$. $wR_2 = \{\Sigma[w(F_o^2 - F_c^2)^2]/\Sigma[w(F_o^2)^2]\}^{1/2}$; $w = 1/[\sigma^2(F_o^2) + (aP)^2 + bP]$ where a is 0.0086, b is 5.1983 and P is $[2F_c^2 + \text{Max}(F_o^2, 0)]/3$.

https://doi.org/10.1180/minmag.2017.081.013 Published online by Cambridge University Press

13.01, As_2O_5 63.22, H_2O 3.30, total 100 wt.%. The Gladstone-Dale compatibility $1 - (K_p/K_c)$ for the empirical formula is 0.004 in the range of superior compatibility (Mandarino, 2007).

X-ray crystallography and structure refinement

Both powder and single-crystal X-ray diffraction studies were carried out using a Rigaku R-Axis Rapid II curved imaging plate microdiffractometer, with monochromatic Mo*Kα* radiation. For the powder diffraction study a Gandolfi-like motion on the φ and ω axes was used to randomize the sample and observed *d*-values and intensities were derived by profile fitting using *JADE 2010* software (Materials Data, Inc.). The powder data presented in Table 3 show good agreement with the pattern calculated from the structure determination. Unit-cell parameters refined from the powder data using *JADE 2010* with whole pattern fitting are $a = 12.183(5)$, $b = 12.506(6)$, $c = 6.802(5)$ Å, $\beta = 112.803(13)°$ and $V = 955.4(9)$ Å^3.

The *Rigaku CrystalClear* software package was used for processing the structure data, including the application of an empirical multi-scan absorption correction using *ABSCOR* (Higashi, 2001). The structure was solved using *SIR2011* (Burla *et al.*, 2012). *SHELXL-2013* (Sheldrick, 2015) was used for the refinement of the structure. The location of all non-hydrogen atom sites was straightforward and atom coordinates were then transformed to be consistent with the standardized atom coordinates for alluaudite-group structures (Krivovichev *et al.*, 2013). (Note that the atom coordinates and O atom assignments for canutite were not reported using this standardized approach.) The *A* site was assigned full occupancy by Na. The *M*1 and *M*2 sites were refined with joint occupancies by Mn and Mg, yielding *M*1: $Mn_{0.748}Mg_{0.252}$ and *M*2: $Mn_{0.443}Mg_{0.557}$. A difference-Fourier map revealed the location of the H atom corresponding to the O2···O4 hydrogen bond. The data collection and refinement details are given in Table 4, atom coordinates and displacement parameters in Table 5, selected bond distances in Table 6 and a bond valence analysis in Table 7.

Description of the structure

Magnesiocanutite is a member of the alluaudite group and is isostructural with compounds with the protonated alluaudite-type structure, including the

TABLE 5. Atom coordinates and displacement parameters (Å^2) for magnesiocanutite.

	x/a	*y/b*	*z/c*	U_{eq}	U^{11}	U^{22}	U^{33}	U^{23}	U^{13}	U^{12}
A(Na)	0	–0.0103(3)	1/4	0.0458(9)	0.0219(16)	0.093(3)	0.0204(16)	0	0.0057(13)	0
*M*1*	0	0.28224(8)	1/4	0.01614(4)	0.0158(7)	0.0162(6)	0.0167(7)	0	0.0068(5)	0
*M*2*	0.29203(8)	0.65987(7)	0.37797(14)	0.0135(4)	0.0147(6)	0.0113(5)	0.0155(6)	0.0006(3)	0.0072(4)	0.0006(3)
As1	0	0.69083(5)	1/4	0.01527(19)	0.0169(3)	0.0144(3)	0.0125(3)	0	0.0036(3)	0
As2	0.21940(4)	0.88691(3)	0.11470(6)	0.01458(16)	0.0173(3)	0.0127(3)	0.0132(3)	–0.00007(15)	0.0054(2)	0.00009(17)
O1	0.4640(3)	0.7337(2)	0.5293(4)	0.0188(7)	0.0163(15)	0.0235(16)	0.0147(15)	–0.0047(12)	0.0041(13)	–0.0001(13)
O2	0.1129(3)	0.6077(2)	0.2654(5)	0.0183(7)	0.0148(15)	0.0126(15)	0.0272(18)	0.0009(12)	0.0079(13)	0.0026(12)
H	0.114(5)	0.517(4)	0.288(7)	0.027						
O3	0.3443(3)	0.6757(2)	0.1211(4)	0.0184(7)	0.0215(17)	0.0190(16)	0.0141(16)	–0.0016(12)	0.0062(13)	–0.0043(12)
O4	0.1336(3)	0.4110(2)	0.3336(5)	0.0206(7)	0.0173(16)	0.0168(15)	0.0303(18)	0.0006(13)	0.0123(14)	0.0036(12)
O5	0.2139(3)	0.8142(2)	0.3164(4)	0.0162(7)	0.0183(16)	0.0181(15)	0.0128(15)	0.0044(11)	0.0068(13)	0.0002(12)
O6	0.3515(3)	0.5038(2)	0.4029(5)	0.0194(7)	0.0197(17)	0.0164(15)	0.0212(18)	0.0012(12)	0.0069(14)	–0.0022(12)

* Refined occupancies: *M*1: Mn/Mg = 0.748/0.252(8); *M*2: Mn/Mg = 0.443/0.557(6).

https://doi.org/10.1180/minmag.2017.081.013 Published online by Cambridge University Press

TABLE 6. Selected bond distances (Å) and angles (°) for magnesiocanutite.

A–O6 (×2)	2.356(3)	*M*1–O4 (×2)	2.204(3)
A–O6 (×2)	2.435(3)	*M*1–O3 (×2)	2.206(3)
A–O3 (×2)	2.915(4)	*M*1–O1 (×2)	2.206(3)
A–O1 (×2)	3.122(4)	<*M*1–O>	2.205
A–O5 (×2)	3.309(4)		
<*A*–O>	2.827	*M*2–O6	2.066(3)
		*M*2–O3	2.101(3)
As1–O1 (×2)	1.684(3)	*M*2–O5	2.120(3)
As1–O2 (×2)	1.700(3)	*M*2–O2	2.122(3)
<As–O>	1.692	*M*2–O5	2.143(3)
		*M*2–O1	2.156(3)
As2–O5	1.675(3)	<*M*2–O>	2.118
As2–O6	1.679(3)		
As2–O3	1.682(3)		
As2–O4	1.720(3)		
<As–O>	1.689		

Hydrogen bond

D–H	*d*(D–H)	*d*(H···A)	<DHA	*d*(D···A)	A
O2–H	1.14(5)	1.37(6)	171(6)	2.497(4)	O4

minerals canutite, $NaMn_3[AsO_4]_2[AsO_2(OH)_2]$ (Kampf *et al.*, 2014*a*), o'danielite, $NaZn_3[AsO_4][AsO_3(OH)]_2$ (Keller and Hess, 1988) and groatite, $NaCaMn_2[PO_4][PO_3(OH)]_2$ (Cooper *et al.*, 2009). The general formula of these phases is $AM1M2_2[T1O_4][T2O_3(OH)]_2$ {*T* = P, As}, where the *M*1 and *M*2 octahedra link by edge-sharing to form staggered chains, *T*1 and *T*2 tetrahedra cross-link the chains, and *A* cations occupy large channel sites (Fig. 3).

The structure refinement for magnesiocanutite clearly indicates that Mn and Mg can both occupy the *M*1 and *M*2 sites, but that there is a distinct preference of Mn for the *M*1 site and Mg for the *M*2 site. Although the small amount of Co and Cu indicated in the chemical analysis was not incorporated into the structure refinement, we included these in an analysis of the *M*1 and *M*2 site occupancies using the program *OccQP* (Wright *et al.*, 2001). This program uses quadratic equations in a constrained least-squares formulation to optimize occupancy assignments based upon site scattering, chemical composition, charge balance, bond valence and cation–anion bond lengths. Assuming full occupancies and using the chemical analytical values for Mn, Mg, Co and Cu, this analysis indicated the *M*1 site to

TABLE 7. Bond-valence analysis for magnesiocanutite. Values are expressed in valence units.

	O1	O2	O3	O4	O5	O6	Σ_c
A(Na)	0.03 ×2→		0.05 ×2→		0.02 ×2→	0.22 ×2→ 0.18 ×2→	1.00
*M*1	0.31 ×2→		0.31 ×2→	0.31 ×2→			1.86
*M*2	0.32	0.36	0.38		0.36 0.33	0.41	2.16
As1	1.25 ×2→	1.20 ×2→					4.90
As2			1.26	1.13	1.29	1.27	4.95
Σ_a	1.91	1.56	2.00	1.44	2.00	2.08	

Multiplicities indicated by ×2→; bond strengths based upon refined Mn/Mg site occupancies; Na^+–O bond-valence parameters are from Wood and Palenik (1999); other bond-valence parameters are from Brown and Altermatt (1985); hydrogen-bond donor-acceptor contributions for O2···O4 are not included.

https://doi.org/10.1180/minmag.2017.081.013 Published online by Cambridge University Press

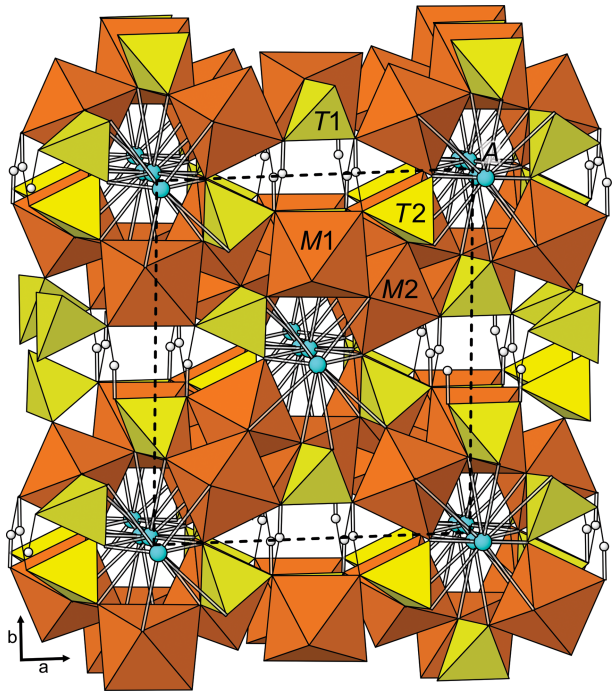

FIG. 3. The crystal structure of magnesiocanutite viewed slightly canted down [001]. Unit cell shown by dashed line. *A*–O and O–H bonds shown as sticks. Hydrogen bonds shown as thin solid lines.

be occupied by 0.784 Mn and 0.216 Mg and the *M*2 site to be occupied by 0.350 Mn, 0.518 Mg, 0.056 Co and 0.076 Cu, providing the structurally based empirical formula $Na(Mn_{0.78}Mg_{0.22})_{\Sigma 1.00}(Mg_{1.04}Mn_{0.70}Cu_{0.15}Co_{0.11})_{\Sigma 2.00}[AsO_4]_2[AsO_2(OH)_2]$.

In the structure of canutite and other protonated alluaudite-type minerals, O4 [part of *T*2 (As2) tetrahedron] is an OH group forming a hydrogen bond to O2 [part of *T*1 (As1) tetrahedron]. An interesting feature of the magnesiocanutite structure refinement is that the H atom position appears to be closer to O2 than to O4, O2–H = 1.14 and O4–H = 1.37 Å; however, it is worth noting that there is also a residual electron density closer to O2. The very short O2–O4 distance is typical for a symmetrical hydrogen bond, although in this case, the bond is somewhat asymmetrical. The bond-valence sums for O2 and O4 without the H contributions are 1.56 and 1.44 valence units, respectively, consistent with such a hydrogen bond character.

Acknowledgements

Reviewers Sergey Krivovichev, Igor Pekov and Joel Grice and Structures Editor Peter Leverett are thanked for their constructive comments on the manuscript. A portion of this study was funded by the John Jago Trelawney Endowment to the Mineral Sciences Department of the Natural History Museum of Los Angeles County.

References

Brown, I.D. and Altermatt, D. (1985) Bond-valence parameters from a systematic analysis of the inorganic crystal structure database. *Acta Crystallographica*, **B41**, 244–247.

Cooper, M.A., Hawthorne, F.C., Ball, N.A., Ramik, R.A. and Roberts, A.C. (2009) Groatite, $NaCaMn_2^{2+}(PO_4)[PO_3(OH)]_2$, a new mineral species of the alluaudite group from the Tanco pegmatite, Bernic Lake, Manitoba, Canada: description and crystal structure. *Canadian Mineralogist*, **47**, 1225–1235.

Gunter, M.E., Bandli, B.R., Bloss, F.D., Evans, S.H., Su, S.C. and Weaver, R. (2004) Results from a McCrone spindle stage short course, a new version of EXCALIBR, and how to build a spindle stage. *The Microscope*, **52**, 23–39.

Gutiérrez, H. (1975) *Informe sobre una rápida visita a la mina de arsénico nativo, Torrecillas*. Instituto de Investigaciones Geológicas, Iquique, Chilie.

Higashi, T. (2001) *ABSCOR*. Rigaku Corporation, Tokyo.

https://doi.org/10.1180/minmag.2017.081.013 Published online by Cambridge University Press

Kampf, A.R., Sciberras, M.J., Williams, P.A., Dini, M. and Molina Donoso, A.A. (2013*a*) Leverettite from the Torrecillas mine, Iquique Provence, Chile: the Co-analogue of herbertsmithite. *Mineralogical Magazine*, **77**, 3047–3054.

Kampf, A.R., Nash, B.P., Dini, M. and Molina Donoso, A. A. (2013*b*) Magnesiokoritnigite, $Mg(AsO_3OH)\cdot H_2O$, from the Torrecillas mine, Iquique Province, Chile: the Mg-analogue of koritnigite. *Mineralogical Magazine*, **77**, 3081–3092.

Kampf, A.R., Mills, S.J., Hatert, F., Nash, B.P., Dini, M. and Molina Donoso, A.A. (2014*a*) Canutite, $NaMn_3[AsO_4]_2[AsO_2(OH)_2]$, a new protonated alluaudite-group mineral from the Torrecillas mine, Iquique Province, Chile. *Mineralogical Magazine*, **78**, 787–795.

Kampf, A.R., Nash, B.P., Dini, M. and Molina Donoso, A. A. (2014*b*) Torrecillasite, $Na(As,Sb)_4^{3+}O_6Cl$, a new mineral from the Torrecillas mine, Iquique Province, Chile: description and crystal structure. *Mineralogical Magazine*, **78**, 747–755.

Kampf, A.R., Nash, B.P., Dini, M. and Molina Donoso, A.A. (2016*a*) Chongite, $Ca_3Mg_2(AsO_4)_2(AsO_3OH)_2\cdot 4H_2O$, a new arsenate member of the hureaulite group from the Torrecillas mine, Iquique Province, Chile. *Mineralogical Magazine*, **80**, 1255–1263.

Kampf, A.R., Nash, B.P., Dini, M. and Molina Donoso, A. A. (2016*b*) Gajardoite, $KCa_{0.5}As_4^{3+}O_6Cl_2\cdot 5H_2O$, a new mineral related to lucabindiite and torrecillasite from the Torrecillas mine, Iquique Province, Chile. *Mineralogical Magazine*, **80**, 1265–1272.

Kampf, A.R., Mills, S.J., Nash, B.P., Dini, M. and Molina Donoso, A.A. (2017*a*) Currierite, $Na_4Ca_3MgAl_4(AsO_3OH)_{12}\cdot 9H_2O$, a new acid arsenate with ferrinatrite-like heteropolyhedral chains from the Torrecillas mine, Iquique Province, Chile. *Mineralogical Magazine*, **81**, 1141–1149.

Kampf, A.R., Nash, B.P., Dini, M. and Molina Donoso, A. A. (2017*b*) Juansilvaite, $Na_5Al_3[AsO_3(OH)]_4[AsO_2(OH)_2]_2(SO_4)_2\cdot 4H_2O$, a new arsenate-sulfate from the Torrecillas mine, Iquique Province, Chile. *Mineralogical Magazine*, **81**, 619–628.

Keller, P. and Hess, H. (1988) Die kristallstrukturen von O'Danielit, $Na(Zn,Mg)_3H_2(AsO_4)_3$, und Johillerit, $Na(Mg,Zn)_3Cu(AsO_4)_3$. *Neues Jahrbuch für Mineralogie, Monatshefte*, **1988**, 395–404.

Krivovichev, S.V., Vergasova, L.P., Filatov, S.K., Rybin, D.S., Britvin, S.N. and Ananiev, V.V. (2013) Hatertite, $Na_2(Ca,Na)(Fe^{3+},Cu)_2(AsO_4)_3$, a new alluaudite-group mineral from Tolbachik fumaroles, Kamchatka peninsula, Russia. *European Journal of Mineralogy*, **25**, 683–691.

Mandarino, J.A. (2007) The Gladstone–Dale compatibility of minerals and its use in selecting mineral species for further study. *Canadian Mineralogist*, **45**, 1307–1324.

Pouchou, J.-L. and Pichoir, F. (1991) Quantitative analysis of homogeneous or stratified microvolumes applying the model "PAP." Pp. 3l–75 in: *Electron Probe Quantitation* (K.F.J. Heinrich and D.E. Newbury, editors). Plenum Press, New York.

Sheldrick, G.M. (2015) Crystal structure refinement with SHELXL. *Acta Crystallographica*, **C71**, 3–8.

Wood, R.M. and Palenik, G.J. (1999) Bond valence sums in coordination chemistry. Sodium-oxygen complexes. *Inorganic Chemistry*, **38**, 3926–3930.

Wright, S.E., Foley, J.A. and Hughes, J.M. (2001) Optimization of site occupancies in minerals using quadratic programming. *American Mineralogist*, **85**, 524–531.

https://doi.org/10.1180/minmag.2017.081.013 Published online by Cambridge University Press